Jurnal Teknologi, 32(F): 93–101

THE PRACTICAL USE OF RESISTANCE MODELING TO INTERPRET THE GAS SEPARATION PROPERTIES OF HOLLOW FIBER MEMBRANES

AHMAD FAUZI ISMAIL[1] & SIMON J. SHILTON[2]

Abstract. A simple resistance modeling methodology is presented for gas transport through asymmetric polymeric membranes. The methodology allows fine structural properties such as active layer thickness and surface porosity, to be determined from experimental gas permeation data. This paper, which could be regarded as a practical guide, shows that resistance modeling, if accompanied by realistic working assumptions, need not be difficult and can provide a valuable insight into the relationships between the membrane fabrication conditions and performance of gas separation membranes.

Key Words: Hollow fiber membranes, gas separation properties, resistance modeling, fine structural details

1.0 INTRODUCTION

Knowledge of fine structural details at the microscopic level is important in a membrane development as it allows more complete understanding of the relationships between fabrication conditions and membrane performance. Such knowledge could be acquired through resistance modeling [1-6].

Resistance modeling involves the construction of an electrical resistance analogue to represent gas permeation. Each resistance is expressed in term of an appropriate flow equation. A parameter fit exercise using experimental data can then yield structural details such as active layer thickness and surface porosity.

A major breakthrough in the fabrication of gas separation membranes occurred in the early 1980's. Hines and Tripodi [7,8] pioneered the production of polysulfone hollow fiber membranes with acceptable flux and selectivity. They employed a silicone coating technique to repair defects in the membrane wall and introduced resistance modeling to rationalize the coating process.

[1] Corresponding author: Membrane Research Unit, Faculty of Chemical and Natural Resources Engineering, Universiti Teknologi Malaysia, 81310 UTM Skudai, Johor Darul Ta'zim.

[2] Department of Chemical and Process Engineering, University of Strathclyde, Scotland, United Kingdom.

Fouda *et al.* [9] introduced a more realistic resistance approach called the *Wheatstone bridge model* in order to fit actual gas permeation results to possible membrane structures. A modified version of the *Wheatstone bridge model* was used by Shilton *et al.* [10]. They explicitly incorporated an expression for *Knudsen diffusion* and were able to predict the pore size as well as other structural parameters from experimental permeation data. The model also showed the ability to estimate the intrinsic selectivity of the solid polymer within the membrane and correlated it with the rheological conditions during fabrication.

The solution of a resistance model is essentially based on an *n*-dimensional parameter fit exercise and, as such, convergence difficulties can be encountered. In fact, the more sophisticated the model, i.e. the greater the number of parameters, the more capricious its behaviour can be. However, accompanied by pragmatic working assumptions, resistance modeling need not be difficult. The current paper presents the use of a practical resistance model where the fine structural properties of hollow fiber membranes are easily determined from gas permeation properties. This structural information can then be used to interpret the relationships between spinning conditions and membrane performance.

2.0 THEORY AND DEVELOPMENT OF RESISTANCE MODEL

2.1 Membrane Structure and Resistance Analogues

Schematic structures of uncoated and coated asymmetric membranes, and the corresponding electrical circuit analogues, are shown in Figures 1 and 2,

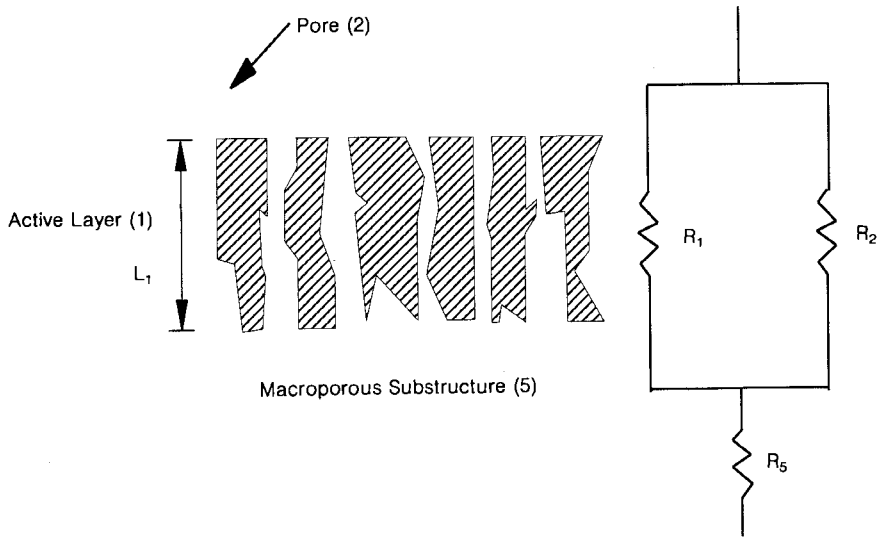

Figure 1 Schematic Diagram of a Uncoated Asymmetric Membrane and the Corresponding Electrical Circuit Analogue

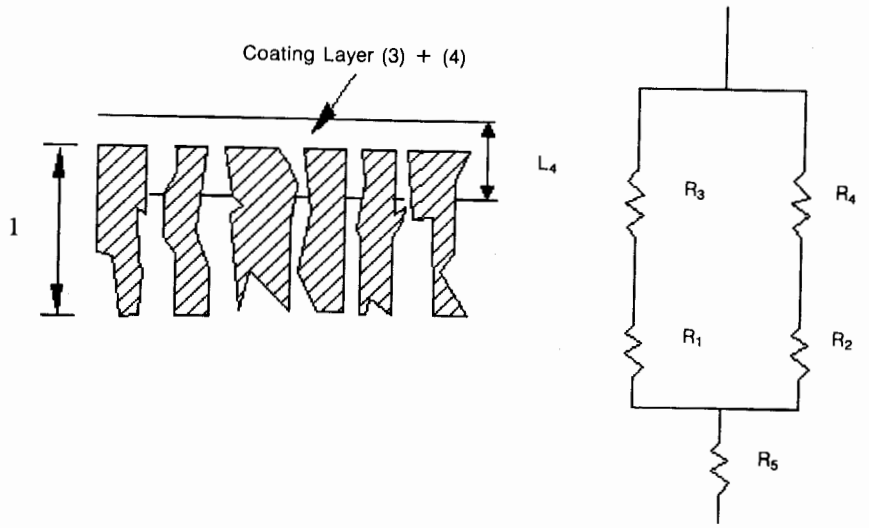

Figure 2 Schematic Diagram of a Coated Asymmetric Membrane and the Corresponding Electrical Circuit Analogue

respectively. Five gas transport regions are identified and hence the existing resistance can be represented by the membrane skin layer (R_1), the pores or imperfections in the skin (R_2), the silicone coating layer (R_3), the silicone pore penetration depth plus overlay height (R_4), and the macroporous substructure (R_5).

2.2 Resistance Model Equations

The overall resistances to gas transport in uncoated (RU) and coated (RC) membranes can be expressed as follow (R_5 is deemed negligible):

$$\frac{1}{RU} = \frac{1}{R_1} + \frac{1}{R_2}, \tag{1}$$

$$\frac{1}{RC} = \frac{1}{R_1 + R_3} + \frac{1}{R_2 + R_4}. \tag{2}$$

The permeation of a gas through a membrane can be described by the pressure-normalized flux, P according to Equation (3):

$$P = Q/(A\Delta p) \tag{3}$$

and the resistance to permeation (R) can be defined as:

$$R = 1/(PA). \tag{4}$$

Using Equations (1) - (4) and flow equations for solution diffusion as well as *Knudsen diffusion*, which have been described elsewhere [10], the following resistance model equations can be stated:

$$P_{\text{iUncoated}} = \frac{\bar{P}_{\text{polymer}} i}{L1} + \frac{8}{3} \frac{1}{\sqrt{2\pi R_0 T M_i}} \frac{r}{L\ 1} A_p, \tag{5}$$

$$P_{\text{iCoated}} = \frac{\bar{P}_{\text{polymer}} i}{L1} + \frac{1}{\left[\frac{L4}{\bar{P}_{\text{coating}}\, i\ A_p}\right] + \left[\frac{3}{8} \sqrt{2\pi R_0 T M_i}\ \frac{L1}{rA_p}\right]} \tag{6}$$

The selectivity α of a membrane towards two gases i and j is simply defined as the ratio of the pressure-normalized fluxes:

$$\alpha_j^i = P_i / P_j \tag{7}$$

2.3 Working Assumptions and Use of Model Equations

When using the resistance model with experimental data, a number of simplifications become necessary and are implicit in the Equations (1) - (6). The simplifications are as follow:

(1) $A_p << 1$, hence the area of the solid polymer equals the membrane area A.
(2) $L_4 << L_1$, hence, on coating, the length of open pore for Knudsen diffusion equals L_1.
(3) On coating, the resistance offered by the outer silicone layer (R_3) is negligible.

Also, in gas separation membranes, surface defects or pores tend to be imperceptible. Electron micrographs do not reveal pores in the fiber walls even at magnification as high as × 10,000, which suggests that pore radius r is not bigger than 100 Å [10]. Therefore, in resistance modeling of gas separation membranes, it is reasonable to assume that r = 100 Å (*Knudsen* flow range). This assumption was employed in this work.

Equations (5) and (6) can be solved using experimentally determined pressure-normalized fluxes for two gaseous penetrants.

As reported previously [11], polysulfone hollow fiber membranes were fabricated using a dry/wet spinning process at two dope extrusion rates [11]. The gas permeation data of these membranes are shown in Tables 1 and 2, respectively and are used as specimen input data. However, the resistance modeling procedure can be used as a general utility that can be applied to any permeation data.

The intrinsic gas permeation properties of the polymer (polysulfone) and coating material (polydimethylsiloxane) for the penetrant gases (CO_2 and CH_4) are given in Table 3.

As early mentioned, the resistance modeling is basically a n-dimensional parameter fit exercise and, as such, is sensitive to the input data. Convergence problems and/or instability may occur with a particular range of input values. These problems were in fact encountered upon the data applying presented in Tables 1 and 2. To overcome such problems, further pragmatic assumptions have to be made.

In Table 1, flow through pores is significant as selectivities are fairly low. Structural properties (L_1 and A_p) were therefore deduced exclusively from uncoated data, using Equation (5) for the two gaseous penetrants.

In the case of Table 2, the selectivities are high for the coated membranes

Table 1 Gas Permeation Properties of Polysulfone Hollow Fiber Membranes Spun at Relatively Low Dope Extrusion Rate[a] [11]

Module	Uncoated		Coated	
	P_{CO_2}[b]	$\alpha_{CH_4}^{CO_2}$	P_{CO_2}	$\alpha_{CH_4}^{CO_2}$
LO1	69.4	1.30	35.4	7.07
LO2	67.0	1.35	39.5	7.70
LO3	45.1	1.83	33.5	4.46
LO4	45.8	2.93	24.2	5.73
LO5	49.4	1.30	32.1	5.97
LO6	43.7	1.22	23.7	4.47
LO7	37.8	2.05	28.3	5.44
LO8	65.2	1.39	68.7	7.81

[a] The spinning dope, which contained 22% (w/w) polysulfone was extruded at a rate of 1.0 cm^3/min. The stretch ratio was maintained at 1.

[b] Pressure-normalized flux $\times 10^6$ (cm^3(STP)/s cm^2 cmHg) measured at 25°C and at a pressure difference of 5 bar.

and many values surpass the recognized polysulfone intrinsic selectivity of 28 for CO_2/CH_4 [12]. Consequently, the flow through pores was regarded to be insignificant in these membranes. The L_1 values were therefore calculated using the following abridged version of Equation (6), using the CO_2 data:

$$P_{\text{i coated}} = \frac{\bar{P}_{\text{polymer}}\ i}{L_1} \tag{8}$$

A_p was in turn calculated from the uncoated pressure-normalized flux for CO_2 using Equation (5).

Further calculations of pore number, (N_p) and distance between pores, (d_p) were found easy to be obtained using Equations (9) and (10):

$$N_p = A_p/(\pi r^2), \tag{9}$$

$$d_p = N_p^{-1/2} \tag{10}$$

Table 2 Gas Permeation Properties of Polysulfone Hollow Fiber Membranes Spun at Relatively High Dope Extrusion Rate[a] [11]

Module	Uncoated		Coated	
	P_{CO_2}[b]	$\alpha_{CH_4}^{CO_2}$	P_{CO_2}	$\alpha_{CH_4}^{CO_2}$
HI1	64.20	1.71	47.50	32.10
HI2	80.70	1.63	38.10	40.20
HI3	88.20	2.18	54.70	13.90
HI4	76.50	2.65	50.50	30.10
HI5	81.30	2.64	50.20	32.70
HI6	79.80	2.31	43.00	34.30
HI7	54.80	3.69	48.80	13.60
HI8	57.50	4.15	51.30	22.30
HI9	62.50	3.50	58.10	41.50

[a] The spinning dope, which contained 22% (w/w) polysulfone was extruded at a rate of 2.5 cm^3/min. The stretch ratio was maintained at 1.

[b] Pressure-normalized flux $\times 10^6$ (cm^3(STP)/s cm^2 cmHg) measured at 25°C and at a pressure difference of 5 bar.

Table 3 Intrinsic Gas Permeation Properties of Polysulfone and Polydimethylsiloxane

Polymer	$\bar{P}_{CO_2}$[a]	$\bar{P}_{CH_4}$	$\alpha_{CH_4}^{CO_2}$
Polysulfone	4.5[b]	0.16	28[b]
Polydimethylsiloxane	3250[c]	950[c]	3.4

[a] Permeability coefficient $\times 10^{10}$ (cm^3(STP)/s cm^2 cmHg).

[b] From Chern *et al.* [12].

[c] From Robb [13].

3.0 RESULTS AND DISCUSSION

The membrane fine structural properties determined using the resistance modeling procedure, shown in Tables 4 and 5, respectively, are for the two sets of hollow fiber membranes. When the details are viewed in correlation the permeation data presented in Tables 1 and 2, a number of observations could be made.

Table 4 Fine Structural Properties Determined by Resistance Modeling - Polysulfone Hollow Fiber Membranes Spun at Relatively Low Dope Extrusion Rate

Module	Thickness of active layer, L_1 (Å)	Surface porosity, A_p (cm^2/cm^2) $\times 10^{-6}$	Pore number, N_p (cm^{-2}) $\times 10^5$	Distance between pores, d_p (Å) $\times 10^5$
LO1	1186	1.136	3.618	1.663
LO2	1191	1.060	3.374	1.721
LO3	1457	0.630	2.006	2.233
LO4	1210	0.318	1.011	3.144
LO5	1661	1.130	3.598	1.667
LO6	1994	1.282	4.080	1.566
LO7	1649	0.528	1.681	2.439
LO8	1193	1.000	3.183	1.772
Average	1442	0.885	2.819	2.026

Table 5 Fine Structural Properties Determined by Resistance Modeling - Polysulfone Hollow Fiber Membranes Spun at Relatively High Dope Extrusion Rate

Module	Thickness of active layer, L_1 (Å)	Surface porosity, A_p (cm^2/cm^2) $\times 10^{-6}$	Pore number, N_p (cm^{-2}) $\times 10^5$	Distance between pores, d_p (Å) $\times 10^5$
HI1	948	0.483	1.537	2.551
HI2	1181	1.535	4.885	1.431
HI3	822	0.820	2.609	1.958
HI4	890	0.652	2.076	2.195
HI5	896	0.848	2.700	1.924
HI6	1046	1.172	3.730	1.637
HI7	922	0.169	0.538	4.311
HI8	877	0.166	0.528	4.352
HI9	775	0.105	0.334	5.473
Average	929	0.661	2.104	2.870

The pressure-normalized flux was found to increase with the increase in the dope extrusion rate. This can be explained by a decrease in active layer thickness as determined by the modeling. Taking a straightforward view, if membranes are defect free, then active layer thickness has little influence on selectivity [14,15]. However, if defects arise, then the thinner the active layer, the more selective is the membrane. The high selectivities of the high dope extrusion rate hollow fibers can be rationalized by the resistance modeling:

these membranes have relatively thin skins and lower surface porosities. Thus, the increase in the dope extrusion rate results in a membrane structure that cause an increase in both pressure-normalized flux and selectivity, two key properties commonly thought to compete rather than increase simultaneously.

It is likely believed that the thinner active layer and lower surface porosity of the high extrusion rate membranes are related to the lower dry gap residence time in the spinning process. The dry gap is considered to be responsible for skin formation [16] and hence the residence time is found to be a critical factor.

Also, many of the higher dope extrusion rate fibers exhibit selectivities beyond the recognized polysulfone intrinsic value of 28 for CO_2/CH_4[12]. This implies that rheological effects are inclusive. The higher levels of shear experienced in the spinneret may orient the polysulfone molecules, causing an enhancement in selectivity. FTIR spectroscopic studies have supported this view [11].

The values of d_p allow visualization of the pore landscape. The values show that if the pores were magnified to 1 cm diameter, the adjacent pores would be about 10 meters away in the low dope extrusion rate membranes and about 15 meters away in the high dope extrusion rate membranes. In view of the uncoated selectivities, this illustrates how damaging a limited number of pinholes can be in gas separation membranes.

4.0 CONCLUSION

In conclusion, this paper has illustrated that resistance modeling can be used in a simple way to deduce fine structural properties of gas separation membranes. The structural information can then be used to help interpret the relationships between fabrication conditions and performance.

REFERENCES

[1] Lundy, K.A., and I. Cabasso. 1989. *Ind. Eng. Res.* 28: 742.
[2] Ashworth, A.J. 1992. *J. Membr. Sci.* 71: 169.
[3] Marchese, J., N. Ochoa and C. Pagliero. 1995. *J. Chem. Tech. Biotechnol.* 63: 329.
[4] He, G., X. Huang, R. Xu and B. Zhu. 1996. *J. Membr. Sci.* 118: 1.
[5] Karode, S.K., V.S. Patwardhan and S.S. Kulkarni. 1996. *J. Membr. Sci.* 114: 157.
[6] Karode, S.K., and S.S. Kulkarni. 1997. *J. Membr. Sci.* 127: 131.
[7] Henis, J.M.S., and M.K. Tripodi. 1980. *Sep. Sci. and Technol.* 15: 1059.
[8] Henis, J.M.S., and M.K. Tripodi. 1981. *J. Membr. Sci.* 8: 233.
[9] Fouda, A., Y. Chen, J. Bai and T. Matsuura. 1991. *J. Membr. Sci.* 64: 263.
[10] Shilton, S.J., G. Bell and J. Ferguson. 1996. *Polymer.* 37: 485.
[11] Ismail, A.F., S.J. Shilton, I.R. Dunkin and S.L. Gallivan. 1997. *J. Membr. Sci.* 126: 133.
[12] Chern, R.T., W.J. Koros, H.B. Hopfenberg and V.T. Stannett. 1985. In D.R. Lloyd (Ed.), Materials Science of Synthetic Membranes, A.C.S. Symp. Ser., 25-46.
[13] Robb, W.L. 1967. *Ann. N.Y. Acad. Sci.* 146: 119.

[14] Li, S.G. 1994. Preparation of hollow fiber membranes for gas separation, *PhD Thesis*. University of Twente.
[15] Koops, G.H., J.A.M. Nolten, M.H.V. Mulder and C.A. Smolders. 1994. *J. Appl. Polym. Sci.* 53: 1639.
[16] Pinnau, I. and W.J. Koros. 1993. *J. Polym. Sci.: Part B: Polym. Physics.* 31: 419.

SYMBOLS

A	Membrane surface area	(cm^2)
A_p	Fraction of membrane surface area that is pores (surface porosity)	(cm^2/cm^2)
dp	distance between pores	(Å)
L	Thickness	(Å)
M	Molecular Weight	(g/mol)
N_p	Number of pores per unit membrane surface area	(cm^{-2})
Δp	Pressure difference	(cmHg)
P	Permeability Coefficient	(cm^3(STP)cm/s cm^2 cmHg)
P	Pressure-normalized flux	(cm^3(STP)/s cm^2 cmHg)
Q	Flowrate	(cm^3(STP)/s or moles/s)
R_0	Universal Gas Constant	(J/mole K)
R	Resistance to Gas Permeation	((s cmHg)/cm^3(STP))
R	Radius of pore	(Å)
T	Temperature	(K)
α	Selectivity	(–)

CLASSIFICATION/SUBSCRIPTS

1	Membrane active layer
2	Pore
3	Silicone coating layer
4	Silicone pore overlay plus penetration
5	Macroporous substructure
U	Uncoated
C	Coated
i	Component i (CO_2)
j	Component j (CH_4)